INL/EXT-07-13386

Feasibility Study for an Autonomous UAV – Magnetometer System

Final Report on SERDP SEED 1509:2206

Roelof Versteeg
Mark McKay
Matt Anderson
Ross Johnson
Bob Selfridge
Jay Bennett

September 2007

The INL is a U.S. Department of Energy National Laboratory
operated by Battelle Energy Alliance

INL/EXT-07-13386

Feasibility Study for an Autonomous UAV – Magnetometer System

Roelof Versteeg[1]
Mark McKay[1]
Matt Anderson[1]
Ross Johnson[2]
Bob Selfridge[3]
Jay Bennett[4]

[1]Idaho National Laboratory
[2]Geometrics, Inc.
[3]U.S. Army Corps of Engineers
[4]Ecosystem Evaluation and Engineering Division, Environmental Laboratory

September 2007

Idaho National Laboratory
Idaho Falls, Idaho 83415

Prepared for the
U.S. Department of Defense
Under DOE Idaho Operations Office
Contract DE-AC07-05ID14517

Table of contents

1 Executive Summary

Large areas across the United States are potentially contaminated with UXO, with some ranges encompassing tens to hundreds of thousands of acres. Technologies are needed which will allow for cost effective wide area scanning with 1) near 100 % coverage and 2) near 100 % detection of subsurface ordnance or features indicative of subsurface ordnance.

The current approach to wide area scanning is a multi-level one, in which medium altitude fixed wing optical imaging is used for an initial site assessment. This assessment is followed with low altitude manned helicopter based magnetometry followed by surface investigations using either towed geophysical sensor arrays or man portable sensors. In order to be effective for small UXO detection, the sensing altitude for magnetic site investigations needs to be on the order of 1 – 3 meters. These altitude requirements means that manned helicopter surveys will generally only be feasible in large, open and relatively flat terrains. While such surveys are effective in mapping large areas relatively fast there are substantial mobilization/demobilization, staffing and equipment costs associated with these surveys (resulting in costs of approximately $100-$150/acre). Surface towed arrays provide high resolution maps but have other limitations, e.g. in their ability to navigate rough terrain effectively. Thus, other systems are needed allowing for effective data collection. An UAV (Unmanned Aerial Vehicle) magnetometer platform is an obvious alternative. The motivation behind such a system is that it would be safer for the operators, cheaper in initial and O&M costs, and more effective in terms of site characterization.

However, while UAV data acquisition from fixed wing platforms for large (> 200 feet) stand off distances is relatively straight forward, a host of challenges exist for low stand-off distance (~ 6 feet) UAV geophysical data acquisition. The objective of SERDP SEED 1509:2006 was to identify the primary challenges associated with a low stand off distance autonomous UAV magnetometer platform and to investigate whether these challenges can be resolved successfully such that a successful UAV magnetometer platform can be constructed.

The primary challenges which were identified and investigated include:

1. The feasibility of assembling a payload package which integrates magnetometers, accurate positioning systems (DGPS, height above ground measurement), obstacle avoidance systems, power infrastructure, communications and data storage as well as auxiliary flight controls
2. The availability of commercial UAV platforms with autonomous flight capability which can accommodate this payload package
3. The feasibility of integrating obstacle avoidance controls in UAV platform control
4. The feasibility of collecting high quality magnetic data in the vicinity of an UAV.

Our efforts in investigating these challenges included (1) a payload evaluation; (2) evaluation of the availability and performance of commercially available autonomous UAV systems; (3) analysis of the requirements posed by obstacle avoidance and an evaluation of whether these requirements can realistically be accommodated in an autonomous UAV and (4) a series of ground based noise tests using a realistic UAV - magnetometer combination. The outcome of each of these efforts is described in detail in subsequent sections. Based on the results obtained from our investigations we conclude that the challenges associated with construction of an effective autonomous UAV magnetometer platform can be resolved successfully and that construction of a successful autonomousUAV magnetometer platform is thus feasible. In section 7 we discuss the potential performance of such a platform compared to currently existing manned platforms and the proposed next steps toward the creation of an autonomous UAV helicopter magnetometer platform.

2 Challenges for an effective UAV Helicopter magnetometer system

2.1 Background: Helicopter based UXO detection

The use of helicopter based UXO detection using magnetic sensors started in the US in 1994. Efforts in this area have resulted in a relatively mature technology. There is agreement about the best design (see the work of (Gamey and Mahler 1999) who concluded that a mounted sensor performed significantly better than towed sensors). There are also increasingly sophisticated acquisition systems which collect data from multiple magnetometers at high sampling rates (~100 Hz), and associated with these acquisition systems are highly accurate positioning systems and sophisticated semi automated data interpretation schemes (Salem, Gamey et al. 2001). A good review of these efforts can be found in (Doll, Gamey et al. 2001).

Two helicopter based systems have been developed over the past years in the USA, the ORAGS (Oak Ridge Airborne Geophysical System) systems developed by Oakridge National Lab (Doll, Gamey et al. 2001; Gamey, Doll et al. 2003) and the MTADS (Multi-sensor Towed Array Detection System) system developed by the Naval Research Laboratory (Nelson, Wright et al. 2004). Both systems are similar in design (figure 2.1), consisting of a boom equipped with a number of cesium vapor magnetometers mounted in the front of a manned helicopter. The ORNL system has 8 magnetometers mounted at 1.75 meter spacing, while the NRL system has 7 magnetometers mounted at 1.5 meter spacing. Note that several versions of the ORNL have been developed over the years with different configurations (e.g. the Hammerhead Array (Doll, Gamey et al. 2001) and the Vgrad system (Gamey, Doll et al. 2003)).

Figure 2.1 MTADS Systems from NRL (left)(Nelson, Wright et al. 2004) and ORAGS-VGrad system from ORNL (right) (Gamey, Doll et al. 2003)

These systems have successfully been used to map and characterize UXO distributions on several sites including the Badlands Bombing Range in 2000 (Doll, Gamey et al. 2001), and Isleta Pueblo (Albuquerque, NM) in 2003 (Nelson, Wright et al. 2004). They have

demonstrated the capability to assess open, flat terrain and detect large individual ordnance items in locations where sensor height can be maintained at very low above ground altitudes (1-2 meters).

The performance of both of these systems is relatively similar: they fly at between 1 and 3 meters above the ground surface, they fly at speeds of about 10-20 meters a second, they collect data from each sensor at about 60-100 Hz, and they both collect a swath of data at a time. The area covered by these systems is in the order of 30-50 acres/hour. Positioning of the sensor data is provided by RTK DGPS, with a reported accuracy of post acquisition positioning of each sensor of 5 cm and a conformance to a predefined flight path on the order of a meter. However, these systems have several characteristics which have prevented their broad application to many sites contaminated with UXO. These characteristics include:

(1) **System and O&M cost**. These include both the cost of the initial system (put by (Nelson, Wright et al. 2004) at about $400K) and the cost of system deployment and operating costs of between $100 and $175 per acre. A significant component of this cost is associated with the helicopter and the pilot, and the need to have onsite geophysical experts for data interpretation. Extrapolation of this cost to the 50 million acres yields a total assessment cost of several billion dollars.

(2) **Site limitations.** The need to fly low is imposed by the need to detect UXO signatures. However, safety considerations only allow this for open, flat areas. In sites with significant topography (or even gently undulating terrain) these systems can not maintain the 1-2 meter altitude necessary for good UXO mapping.

(3) **Limitations in ability to perform detailed localized mapping**. The current systems are limited in their ability to detect small ordnance, and cannot "zoom in" on specific areas of interests (also due to limitations in absolute positioning). Thus, these systems do not provide the required ability for 100 % mapping and require additional land based surveys.

While future work on these systems (including addition of electromagnetic sensors) is expected to provide incremental enhancements to these systems, the primary characteristics listed above are not likely to change substantially. The premise underlying our efforts is that the current limitations of airborne magnetometry can be overcome by replacing the current manned helicopter platform by an autonomous UAV helicopter platform. In the remainder of this section we assess the primary challenges associated with such an autonomous UAV helicopter platform

2.2 Primary challenges associated with design and implementation of an effective UAV Helicopter magnetometer system

An ideal UAV Helicopter magnetometer system should allow for the effective and high confidence detection and discrimination of munitions of concern. This should be done by

the acquisition of regularly spaced values of the magnetic field and/or of the gradient of the magnetic field as closely as possible to the munitions of concern. Note that the benefits of proximity for both identification and characterization are well known **(Stanley 2003)** The measured and reported magnetic field will typically differ from the true magnetic field due to a variety of factors, including but not limited to

1. positioning error (ie, we report a datapoint at a different point than where it is truly recorded)
2. sensor related effects
3. magnetic noise induced by the acquisition platform[1]

A basic requirement for an UAV Helicopter magnetometer system is that it can collect this data. Note that the attributes of the specific munitions of concern will determine sensor height and data spacing.In addition there are a number of practical requirements relating to the ability of such a system to carry the requisite payload, to fly autonomously for extended durations, and to avoid possible obstacles in the flightpath.

Thus, the success of an UAV Helicopter magnetometer is subject to the following conditions

1. The ability to design and integrate the requisite payload elements associated with such a system. This is obviously subject to power, size and weight limitations imposed by both the UAV and operational needs. Payload elements would include magnetometers, data storage and communications infrastructure as well as a power infrastructure (either using batteries, on board power generation or some hybrid solution). In addition (dependent on the base capabilities of the UAV) such a payload might need to include Differential GPS, an Inertial Navigation System, laser altimeter and laser avoidance systems.
2. The commercial availability of helicopter UAVs which can operate autonomously and can carry this payload for appropriate flight times.
3. The feasibility of integrating collision avoidance hardware and software in such a manner that a helicopter UAV can fly at elevations of about 1.5 meters at speeds of about ten meters per second.
4. The feasibility of collecting high quality magnetic data on such a platform. This will most likely require both judicious placement of the magnetometer, minimization of noise generating components and post acquisition noise elimination.

The goal of this project was to evaluate whether these conditions could be met and thus whether an UAV Helicopter Magnetometer system would be feasible to construct. In the

[1] It should be noted that the magnetic noise induced by the acquisition platform can to a large extent be eliminated through a two step effort. First, reduction of the magnetic signal associated with the acquisition platform through judicious placement of compensating magnets and second through the processing of the raw values using compensation software. Details on this are provided in a subsequent section.

subsequent sections each of these conditions are discussed in detail, followed by a summary section discussion the overall results and next steps.

3 System components of an UAV Helicopter magnetometer system

3.1 Introduction

An UAV Helicopter magnetometer system will require the mounting of a payload on a UAV Helicopter and the integration of this payload with the UAV infrastructure. In this section we discuss the elements of this payload. Some data which are required for accurate magnetic mapping (for instance, helicopter position and platform yaw, pitch and roll, which are required for correction of the helicopter effect) are required for autonomous flight, and generally will be accessible. Table 3.1 gives a list of components required for effective data acquisition and list which components are expected to be present on the autonomous UAV.

Component	**Present on autonomous UAV**
Magnetometer	No
DC Power	No. Would need to be provided by batteries
Obstacle avoidance sensors	No
GPS	Yes. Precision order of 10 cm
Helicopter orientation sensors (pitch, yaw, roll)	Yes
Data storage	No
Data transmission infrastructure	Yes, potential issues with integration/ available bandwidth
Data acquisition	No. Would need PC104 stack or similar
Data processing capability for obstacle avoidance sensors	No. Would need PC104 stack or similar

Table 3.1 Components required for magnetic data acquisition

Based on table 1 we briefly discuss candidates for each of the components which are not present on an autonomous UAV. The specific relevant specifications of these components (weight, dimension, power consumption and output rates) are summarized in table 3.2. It should be noted that while candidate selection was done based on criteria for minimizing weight, dimension and power it is possible that marginally better candidates exist for for instanceobstacle avoidance sensors and power. However, we do not expect such candidates to significantly affect the total weight/power requirements as the primary contribution to the weight and the power is from the magnetometer.

	weight (grams)	dimensions (mm)	Data rate (kB/second)	Output refresh (hz)	voltage	W
G823A magnetometer						
Sensor + cable	685	140 (length) x 60 (diameter)	3.6 (at 20 Hz)	10-40	24	12
Electronics bottle	985	300 (length) x 65 (diameter)				
Cable between electronics bottle and connector box	1270					
Connector box	246					
Powercable	618					
Total weight (assume modified components have weight of 500 gram)	**2170**					
Obstacle avoidance sensors						
Opti Logic range finder	224	32 x 78 x 84 mm	19	10-1500	7-9	1.8
Video Camera	400	157x36x47 mm	1400-4000	18-48	8-32	2.5
Laser ranger	200	30 x 60 x 40 mm	19.2-500	10-250	8-32	1
Optic Flow sensor	150	40 x 30 x 10 mm	4.5 -1350	10-1500	5-12	1
Pc104 stack	300	100 x 100 x 50 mm			5-12	0.4
Power						
Lithium power pack (24 V, 1300 mAh)	250	40 x 31 x 102				
Lithium power pack (12 V, 1300 mAh)	130	20 x 31 x 102				
Enclosure	300					
Sensor boom	900					
Total weight	3370					

Table 3.2 Basic system components. Total payload package will weigh about 3400 grams. Note that this assumed that some components of the G823A (cable between electronics bottle and connector box, connector box and power cable) can be modified to weigh about 500 grams. Note that the data rates for the obstacle avoidance sensors are ranges, and that most of this data would be processed on board (and thus would not be stored or transmitted).

3.2 Magnetometer

We have selected the Geometrics G823A Magnetometer as our high sensitivity magnetic sensor of choice. These magnetometers are currently used for numerous airborne surveys,

including on the NRL system. Geometrics is currently working on a novel magnetometer as well (the G824/321). The G823A is shown in figure 3.1. It consists of a sensor bottle and an electronics bottle connected by a cable with a configurable length. The sensor outputs data over a serial port at user configurable rates of between 1 to 40 Hz. Per sample the magnetometer has 18 ten bit characters which at 20 Khz results in 3.6 kB/second. At higher sample rates this increases proportionally. The current drain on start up is 1 amp at 24 v per magnetometer. That drops to 400- 500ma within 2 minutes of startup.Thus the actual current drain during operation is 10-12 watts continuous per magnetometer (this is the number used in table 3.2) . The G824/321 will have significantly increased data output rates (up to 1 KHz) and similar or better characteristics as the G823A in terms of magnetic field measurement.

Figure 3.1 G823A unit. This consists of a sensor unit (short wite tube) connected to the electronics unit (long white tube, shown in open condition) This unit is also shown mounted on the helicopter in section 6, figures 6.3 and onward.

3.3 Obstacle avoidance sensors and data processing capability

Details on the obstacle avoidance sensors listed in table 3.2 are provided in section 5. These are

1) Optic Flow
2) Opti Logic Laser Ranger
3) Stereo Camera
4) Laser Distance sensor

These are the obstacle avoidance sensors which are considered the most likely to be implemented on an UAV. Note that - dependent on payload abilities - a Sick Laser could be added to these sensors (see section 5.4.5, which includes an example of a Sick Laser on a helicopter). The power demands for these sensors are included in table 3.2.

However These sensors will require power, and it is assumed that these sensors can utilize the PC104 stack as data processing/transmission infrastructure.

3.4 Data acquisition/processing/storage and transmission

Data acquisition (for the magnetic data) and data processing (for the obstacle avoidance sensors) will require on board computing capabilities. This computing ability could potentially also be used to filter and down sample the magnetic signal, and apply real time compensation correction. For this, the selected solution is an embedded computer which would provide both on board storage, processing power, I/O boards and (if required) even data transmission capabilities. A number of different low power, low weight computing platforms are available which have the required computing and storage power.

On board data storage of all collected magnetic data, of the basic UAV positioning data and of a subset of the data from the obstacle avoidance would be preferable to allow for post processing verification and image enhancement. This would be feasible with currently available flash memory.

In addition to on board storage real time data transmission of navigation information as well as basic magnetic sensor data would be required. For current fixed winged platforms the INL UAV group has experience with standard modems, which can transmit data over distances of over 1 mile without problems. For magnetic sensor data (and a subset of the obstacle avoidance data) a dedicated second modem would be used which can provide a sustained bandwidth of about 100 kb/S. Several commercial systems exist which meet this demand (e.g. the systems manufactured by FreeWave Technologies). These systems typically have significantly longer capabilities than the 1 mile quoted above, but this may need to be tuned to comply with FAA requirements.

3.5 Power infrastructure

All payload components can be run on DC voltage, typically either 12V or 24V. This voltage will need to be provided by batteries. While all components need some power, table 1 shows that the magnetometer demands outweigh by far all the other needs. On board power generation is not really an option, thus power will need to be provided by batteries. While battery technology is evolving, current lithium polymer batteries would provide a good option. Battery power is of course dependent on total operational time. The specs provided in table 1 are for an operational time of 1 hour.

3.6 Enclosure and Boom

The payload elements will need to be packed in an enclosure, and the magnetometer will need to be placed on a boom (figure 3.2) mounted ahead of the helicopter. The specific

configuration of the enclosure and boom are still open. However, assuming that the boom would be constructed of 10 feet of composite rigid pipe (thin walled fiberglass tube), the boom weight would be about 900 grams. The enclosure weight is assumed to be about 300 grams. The dimension of the enclosure would need to be such that all components cand be accommodated (with the magnetometer sensor mounted on the boom). An enclosure diameter of 320 x 160 x 150 mm should be sufficient to hold all components. Such an enclosure can be accommodated between the helicopter skids.

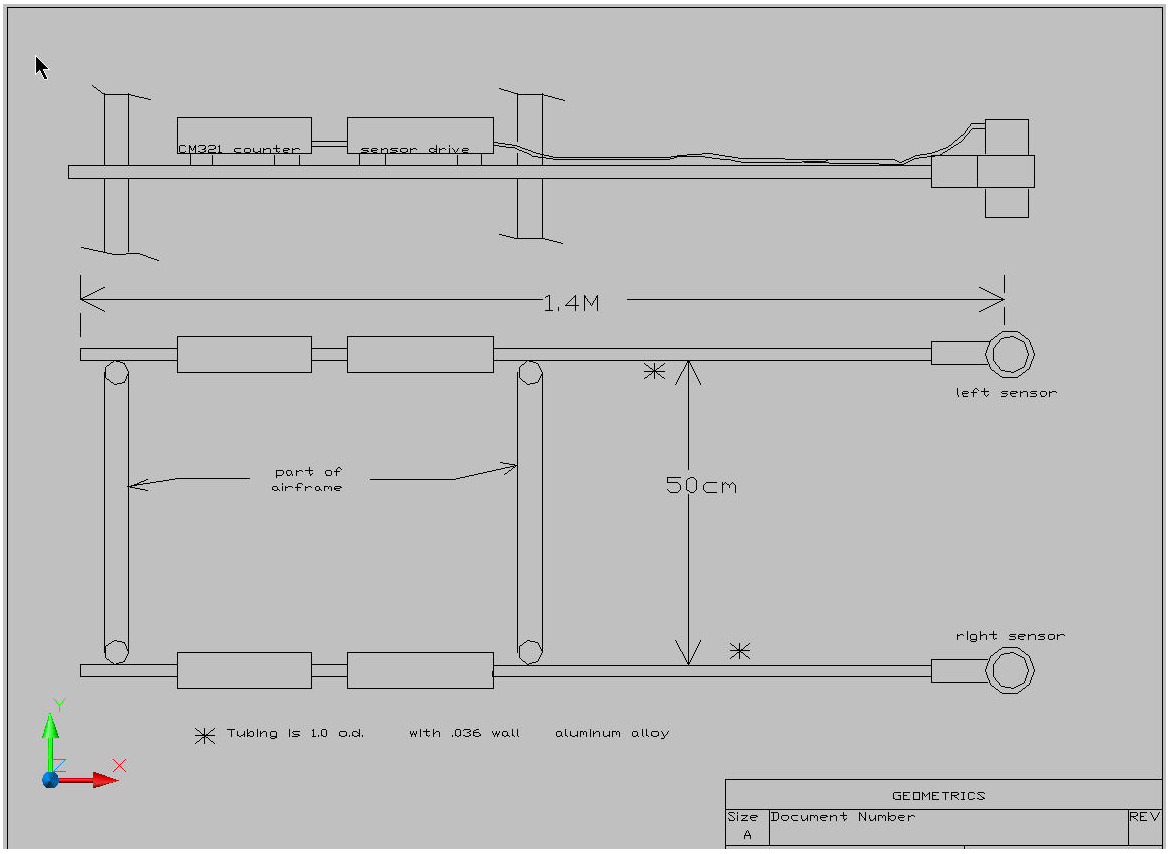

Figure 3.2. Boom design for a two sensor magnetometer. Note that the electronics components for this boom design could be enclosed in an enclosure directly underneath the UAV, and that the center of gravity for the boom could be designed to be underneath the center of gravity for the UAV

3.7 Summary

The minimum payload required for a single magnetometer UAV system will weigh about 3400 grams (about 7.5 lb). The majority of this weight is associated with the

magnetometer. Including multiple magnetometers (e.g. on a boom) and a Sick Laser system for obstacle avoidance (section 5.4.5) would increase this payload to approximately a total of 20-25 lbs. Power requirements for this payload can be met using LiPo (lithium polymer) batteries, which provide an efficient solution to the power problem. On board power generation is not an option.

4 Investigation of commercially available UAV and RC Helicopters

4.1 Introduction

Remotely operated helicopters have been available since the mid 1980s. Due to the complexity of controlling system stability, the first successes in autonomous flight of UAV helicopters only occurred in the late 1990s (Chapuis, Eck et al. 1997; MIT 1998). Since then several commercial platforms have been developed which offer autonomous flight capability. In this section we give a brief overview of several commercially available autonomous and remote controllable helicopters. Table 4.1 provides a side by side comparison of these platforms. Note that while several of the platforms discussed here do not meet the core requirement of autonomous flight or payload they would be useful in the development and refinement of e.g. the obstacle avoidance components of the system. It should be noted that in addition to the commercial systems discussed here multiple (semi) autonomous research UAV helicopters have been developed at universities.

4.2 Yamaha Rmax

The Yamaha RMAX (http://www.yamaha-motor.co.jp/global/industrial/sky/index.html). Built by Yamaha in Japan for agriculture applications, the Rmax (Figure 4.1) is the ultimate workhorse of small unmanned helicopters. The Rmax has three modes of operation; remote piloted, Yamaha Attitude Control System (YACS) assisted control, or full autonomous control. Under manual or remote piloted control the operator flies the helicopter like any other remotely controlled helicopter. With the YACS system activated the computer will hold the helicopter in a stationary hover or in stable flight up to 15km/h. This system is capable of autonomous flight using user defined GPS way points.

Figure 4.1. Yamaha RMAX

4.3 Neural Robotics Autocopter

The Neural Robotics Autocopter family (http://www.neural-robotics.com/) includes several members, including the Autocopter, the Autocopter G (released in February 2007) and the Autocopter XL (scheduled for release in Mid 2007). They all have a common control software which uses a proprietary Neural Network controller to stabilize and fly the system. The AutoCopter can accommodate external disturbance such as winds or a swing load while maintaining accurate position. One unique feature of the AutoCopter is that it does not require a lot of flight training or flight experience. Using the joystick transmitter a pilot can maneuver forward, backward, sideways, and up or down. In autonomous mode, the AutoCopter can fly to GPS waypoints or a grid. The PC/104 based avionics consist of attitude and heading reference, WAAS compatible GPS, ultrasonic altimeter, a barometric pressure sensor, and a heading hold gyro. Payload specifications vary for each Autocopter vary and are shown in table 4,1. The standard Autocopter system is equipped with a 3-axis gyro stabilized camera platform. The platform can be adjusted to accommodate a payload of up to 15 lbs. The platform can also be "fixed" to accommodate applications requiring solid mounted sensors. The current flight time is 30 minute but payload can be traded for additional fuel. An INL owned Autocopter was used for the field tests described in this report. Regarding positioning, in recent results the Autocopter (using a Novatel GPS) was able to hold position within several inches.

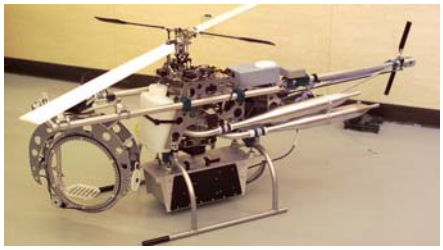

Figure 4.2 Neural Robotics Autocopter

4.4 Bergen R/C Helicopters

Bergen (http://www.bergenrc.com/) makes a number of different R/C (Remote Controlled) Helicopters. These include the (INL owned) Observer and Industrial Twin (Figure 3). These helicopters do not come with built in autonomous flight abilities and require manual control.

Figure 4.3 Bergen Observer R/C Helicopter

4.5 Raptor Cam

The Raptor Cam is a small helicopter. It is based on the Thunder Tiger Raptor 50. It has been upgraded with FMA co-pilot, a thermal sensor used to enhance flight stability (hover control). It is capable of a maximum range of 800 ft. (direct line of sight control). It has a maximum flight time of 20 minutes operating on Nitro fuel and a payload of less than 2 lb. This helicopter is representative of a whole series of similar RC controlled helicopters.

					
Name	RaptorCam	Bergen	AutoCopter	AutoCopter XL	Yamaha Rmax
Payload Capacity	0 – 2lb	5 to 10 lb	15lbs	50 lbs.	60 lbs.
Main Rotor Diameter	53 in	61 to 70 in	72 in	118 in	123 in
Weight	7 lb	16 lb – 18 lb	47.53 lb	51 lb	103 lb
Engine	8cc Nitro	23 to 28 cc Gas	80 cc Gas	120 cc Gas	246 cc Gas
Flight Capability	Manual w/computer assisted stabilization	Manual w/computer assisted stabilization	Manual Semi-autonomous (auto takeoff/landing) Auto hover, stable flight, altitude hold	Manual Semi-autonomous (auto takeoff/landing) Auto hover, stable flight, altitude hold	Manual Semi-Autonomous Full Autonomy
GPS	N/A	N/A	Novatel	Noveatel	YACS
Duration	20 min	30 min	35 min	60 min	60 min
Wind	15 mph	20 mph	20 mph	Not yet known	15+ mph
Cost	$35K	$2.5 to $5K	$30K	$45K	$250K – $1M
Recovery	AutoRotate	AutoRotate	Auto return, Parachute, AutoRotate	Auto return, Parachute, AutoRotate	not available
Range	800 ft	800 ft	2000 ft	2000 ft	?????
Max Altitude	800 ft	800 ft	1000 ft	1000 ft	500 ft
Telemetry	72 MHz up link for flight control 900 MHz Video down link	72 MHz up link for Flight control 2.4 GHz video down link	72 MHz up link 2.4 GHz video down link 900 MHz data down link	72 MHz up link 2.4 GHz video down link 900 MHz data down link	72 MHz up link 2.4 GHz video and data down link
Owner	INEEL	INEEL	INEEL	NRI	Carnegie Mellon University Helicopter Lab & RE^2
Availability	Now	Now	Now	6 months	6 months

Table 4.1 Comparison of commercially available UAV and RC systems. N/A stands for Not applicable: the Raptor Cam and Bergen are not autonomous systems, and thus do not have a standard GPS onboard. The Autocopter XL is still in prototype, so the wind performance is unknown, but is expected to be similar or better to the Autocopter.

4.6 Summary

Currently both the Neural Robotics Autocopter and Yamaha RMAX helicopters meet the specifications for autonomous flight, payload and flight time. It should be noted that the developments of autonomous helicopters is an active field of research, and it is thus reasonable to postulate that the abilities and options for autonomous helicopter flight will increase significantly over the subsequent years.

5 Feasibility of Autonomous obstacle avoidance

5.1 Introduction

As an UAV helicopter-magnetometer system will have to be able to fly at altitudes of about 1-2 meters above ground at speeds of about 1-8 m/s, the ability to collect and integrate knowledge about both terrain elevation, known obstacles (e.g. power poles) and obstacles which would be detected on the fly (e.g. trees) is critical. Thus, a key component for an UAV helicopter-magnetometer system is the ability to have precise positioning (both for flightpath execution and for data acquisition purposes), terrain following abilities and an obstacle avoidance system. In this section we discuss relevant sensors this component. Note that none of these sensors are specific to any rotor air craft, but we have selected sensors based on a rotor-craft main rotor diameter of 10 ft or less. Example potential rotor-craft in this class are, the Yamaha Rmax, or the NRI Autocopter (Figure 5.1). It is anticipated that the rotor-craft will be equipped with autonomous navigation and that the obstacle avoidance sensors will be integrated into the flight avionics. It is also assumed that the low altitude surveys will be conducted at 1 to 2 meters above ground in open areas mostly devoid of large obstacles and that the survey speed will be on the order of 1 to 8 m per second. Note that 8 m/s is the upper range of the speed at which an UAV is expected to work well, and would be valid for flat, open terrains. For complex terrains representative speeds would be in the order of 4-5 m/s.

Figure 5.1. Two target rotor aircraft. Left: Yama Rmax. Right: NRI Autocopter

5.2 Obstacle Avoidance

Obstacle avoidance in unmanned systems is the ability for the machine to recognize that an obstruction is impeding it's progress so that it has the ability, or intelligence, to appropriately respond to that obstruction. For the application at hand, there are two types of obstacles to be avoided:

1) Any object obstructing the desired path of the unmanned rotor-craft system
2) The ground or terrain over which the system is surveying.

For optimal acquisition of magnetic data, the unmanned rotor-craft will need to operate in close proximity to the surface, as such one of the functions of the obstacle avoidance system will be to keep the rotor-craft at a constant distance from the ground or surface. This is often referred to as *terrain following*. While terrain following is not traditionally considered an obstacle impeding the rotor-craft's desired path, gradual or sudden changes in terrain, or even environmental changes, if left uncorrected can impede or terminate progress. If the surveyed surface is treated as an obstacle in close proximity then the system can constantly adapt to the surface variations, correct it's path appropriately and successfully achieve the mapping objective. In the remainder of this section we will thus consider terrain following as an obstacle avoidance challenge.

There are two measurements required for reliable obstacle avoidance; detection and ranging. Object detection sensors are typically those with a "forward look" capability and are able to distinguish finite variations within the field of view (FOV). Some detection sensors have the ability to approximate the radial location of the detected object within it's FOV, but can not identify the range to that object. Typical range sensors can determine distance to an object but without specialized pointing hardware are unable to determine the location of the object within the FOV. In some instances, the combination of motion or two or more sensors can provide a sensor system that can provide both range and direction to a detected object.

Obstacle avoidance sensors can be grouped into either passive or active sensors. **Passive sensors** are not required to emit energy in order to detect an object, instead "receive" existing forms of energy such as light and heat. Sensors in this category can vary greatly and are typically small and low cost. They typically do not have the capability to provide range to the object, but can generally be used to obtain information concerning an object's properties (for instance, whether there is a change in the radial position of an object). **Active sensors** emit energy and expect a return or echo, indicative of the presence of an object. These sensors are also known as time-of-flight (TOF) sensors. TOF measures pulses of energy, typically, Ultrasonic, Radio Frequency, or Laser. The measured time is representative of the twice the separation distance from the object. Active sensors are accurate and reliable to within feet (or sometimes inches) depending on the magnitude of the range to objects. Active sensors often can not provide radial location of the object within it's FOV. Table 5.1 summarizes sensor categories.

Obstacle Detection Sensor Category	Advantages	Disadvantages
Passive	Wide range of sensors	unable to identify range to object
Active	capable of determining the distance to an object	Some active sensors are unable to determine where the object is within a given field of view

Table 5.1: categories of object avoidance sensors

Within each of the sensor categories are several types of sensor technologies that can be used in varying ways to detect objects Passive sensors are typically easier to setup, are less expensive and have fewer moving parts, while active sensors require a higher degree of installation and typically cost more. Tables 5.2 and 5.3 provide details on relevant sensors in the passive and active categories respectively. Sensors which are not directly amenable to obstacle detection are not listed in these tables.

Sensor	Advantages	Disadvantages
Thermal - detects thermal energy	works at night (low to high cost)	sensitivity, high end expensive
Magnetic - detects changes in magnetic fields lines	simple, no moving parts	week signal, require close proximity
Capacitive - detects changes in electric fields (very close proximity)	simple, low cost	short range (<6 in) or contact required
Contact/limit switch/whisker	simple, low cost	requires contact to surface
Optical energy sensors (light diode)	simple, low cost	light sensitive require close proximity
Monocular Camera - small ccd or digital camera, lens variation for different applications	very small and lightweight	susceptible to varying lighting and contrast conditions, not suited for outdoors
Stereo Camera	Works well in varying terrain, can provide range information	Fails in changing light or dark
Optical Flow - small imaging array detects changes in image flow	can identify and provide location of multiple objects	emerging technology

Table 5.2: Passive sensors for object detection

Sensor	Advantages	Disadvantages
Laser	precision and accuracy to object	size, cost, dust,
Laser Distance	Precision and accuracy	size, minimum distance, interface
Laser Altimeter	precision and accuracy	size, minimum distance, interface
Scanning Laser	capable of determining the distance and bearing to an object	Large size, Planar, susceptible to dust, lighting
LADAR (Laser Radar)	capable of imaging obstacle map	large size
Infra Red (IR)	small simple	limited range
Ultrasonic	small, low-cost	limited range, susceptible to noise
Radar	precision and accuracy	large, expensive, interface
Micro Impulse Radar	small, accurate	expensive

Table 5.3: Active sensors for object detection

5.3 Obstacle avoidance sensor selection criteria

The evaluation and rating of potential obstacle avoidance sensors is based on the following criteria:

1) Size and weight: Is the physical size and weight of the sensor such that it allows for easy integration on to a rotor-craft?
2) Cost: Is the cost reasonable for small unmanned rotor-craft?
3) Range: Does the range of the sensor meet the operational requirements?
4) Accuracy: Does the accuracy and resolution of the sensor meet the operational requirements?

Table 5.4 lists sensors that have been evaluated and were scored based on the criteria listed above. Each sensor was given a score from 1 to 3, where 1 = high cost, large size, short range, 2 = mid cost, size or range and 3 = low cost, small size or extended range. The sensors are also grouped according to sensing technology.

Note that while this scoring methodology provides a first indication of suitability, there are some sensors which are clearly inapplicable to the problem at hand (e.g. limit switch,

magnetic sensor, thermal sensor). Thus, for the downselect the results of tables 5.2-5.4 and consideration on the specifics of UAV flight were taken into consideration.

	Sensor	Category	Size	Cost	Range	Accuracy	Score
	Optic Sensor	P	3	3	1	1	8
	Monocular Camera	P	3	3	2	1	9
	Stereo Camera	P	3	2	2	2	9
	Omni Camera	P	2	2	2	2	8
	Optic Flow	P	3	3	2	3	11
	Sick Laser Ranger	A	1	1	2	3	7
	Opti Logic Laser Ranger	A	2	2	3	3	10
	Laser Distance	A	3	2	1	3	9
	Ultrasonic	A	3	3	1	2	9
	Infrared/Thermal	A	3	1	1	1	6
	Radar (Vorad)	A	2	1	2	2	7
	Micro Impulse Radar	A	3	1	2	1	7
	CSC Light Sensitive	P	3	2	1	1	7
	IR emitter/detector	A	3	3	1	1	8
	Magnetic	P	3	2	1	1	7
	Limit/Contact Switch	P	3	3	1	1	8

Table 5.4: Rating of active and passive sensors for object detection. 1 = high cost, large size, short range, 2 = mid cost, size or range and 3 = low cost, small size or extended range. P= Passive, A=Active sensor.

5.4 Proposed Sensors for Obstacle Avoidance

Based on tables 5.2 through 5.4 as well as considerations on the particularities of UAVs five different sensors were selected as candidate sensors. Note that while the score in table 5.4 was used as a first indicator for which sensors to select the overall performance and weight of sensors was taken into detailed consideration for the downselect. As experience has demonstrated that no one single sensor is adequate for all conditions our current recommendation would be to utilize an array of sensors to assure the best obstacle avoidance performance. The recommended sensor array consists of:

1) Optic Flow
2) Opti Logic Laser Ranger
3) Stereo Camera
4) Laser Distance
5) Sick Laser ranger

This selection was made based on the general requirements for what this sensor suite should be able to do. A brief description of each selected sensor is provided below. Note that the Sick Laser Ranger would be a better choice than the opti logic laser ranger as it provides distance over a 180 degree range at a 10 Hz. This sensor has been deployed at UC Berkeley on a Yamaha RMAX. However, the weight of the Sick laser is 4.5 kg, and the SICK laser requires substantial power. Dependent on the rotorcraft platform chosen the power and weight requirements may eliminate the Sick.

5.4.1 Optic Flow sensors

Optic Flow sensors (Figure 5.2) are relatively new to obstacle avoidance. Insect inspired, they rely on the "flow" of image texture or visual motion. Essentially, optic flow is the apparent visual motion that occurs as the sensor moves much like one would see while sitting in a car and were looking out the window. You would see trees, the ground, buildings, etc., appear to move backwards. This motion is optic flow. This motion can also tell you how close you are to the different objects you see. Distant objects like clouds, and mountains move so slowly they appear still. The objects that are closer, such as buildings and trees, appear to move backwards, with the closer objects moving faster than the distant objects. Very close objects, such as grass or small signs by the road, move very fast. The most common usage for optic flow sensors today is in the "optical mouse" used with most desktop computers. The concept of optical flow can be defined, loosely, as the use of texture in images as a source of motion cues.

Optic flow has been shows to be very effective as a means of avoiding obstacles and controlling altitudes. The magnitude and direction of the optic flow is directly related to the speed, orientation and distance to objects within the sensors FOV. Figure 2 below

shows what the optic flow pattern might look like from a rotor-craft flying over a desert terrain. The sensor sees a large optic flow to the right, which is due to the large rock on the left-hand side of this picture. The sensor also sees smaller optic flow patterns in the downward-front direction, due to the ground. Towards it's upper left, it sees no optic flow because this region of the visual field only has the sky. The forward optic flow pattern reveals an obstacle to the right. If the optic flow on the aircraft's right grows larger, then the rotor-craft should turn away.

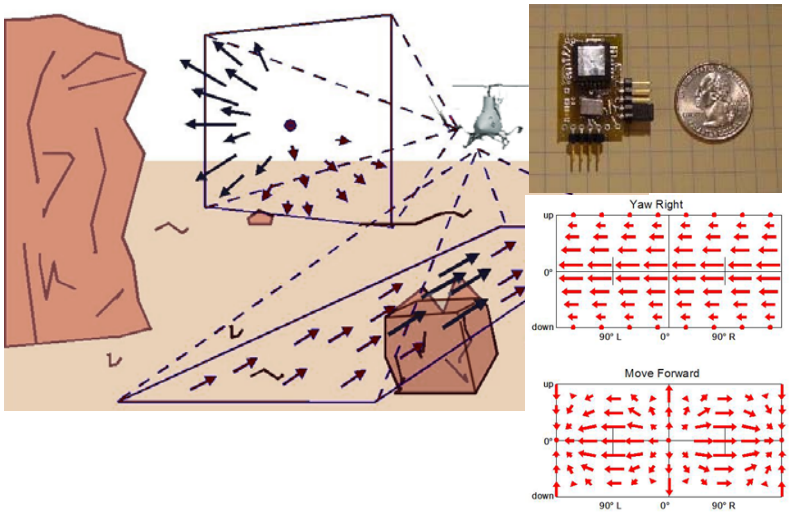

Figure 5.2. Optic flow sensor and an example of how information would look like. Top right: optical flow sensor next to dime for scale.

Flight speed can also be adjusted using optic flow so that the rotor-craft flies slower when in a cluttered environment. If the optic flow on all sides increases beyond a safe limit, the controller should slow down the forward speed until the optic flow is at a more reasonable level.

5.4.2 Opti Logic Laser Ranger

The Opti-Logic RS100/RS400/RS800 units (Figure 5.3) are laser range finding instruments that output measured distance readings to an RS-232 compatible port. The range data can be output as either raw (relative) or calibrated (actual) distances. This information can then be used in several applications. The RS100, RS400, and RS800 units offer similar operation features, with the only difference in the units being the sensitivity to range 100, 400, or 800 yards, respectively.
This sensor is directional with a very narrow FOV. It operates on the principal of time of flight (TOF). The sensor measures the time it takes for a laser pulse to return, and the distance to an object can be simply calculated from this time.

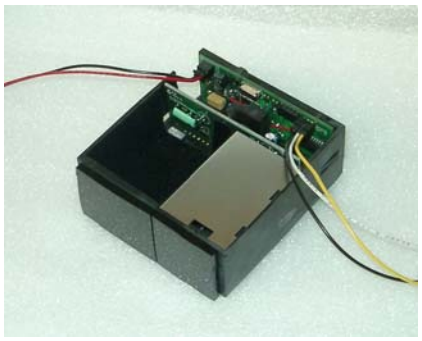

Figure 5.3. Opti Logic Laser Ranger

5.4.3 Stereo Camera

A Stereo Camera is simply two cameras set at a known distance apart. This distance is known as ocular disparity. Ocular disparity in imagery can be used to calculate range to objects within the image. A difficulty in applying stereo vision ranging to autonomous systems is the ability for the onboard navigation system to recognize the correct obstacle. However, for the application at hand, it is anticipated that the FOV will be unobstructed, and that the main challenge will be to do obstacle avoidance (rather than obstacle recognition). Thus, the data from such a system should be able to be used for obstacle avoidance. An example of a stereo camera which could be utilized is Point Grey Research's Stereo Vision camera system (Figure 5.4). These are provided as complete hardware and software packages allowing users to access and control all PGR Stereo Vision camera systems.

Figure 5.4 Point Gray Stereo Vision Camera. This camera has dimensions 160 X 40 X 50 mm, and weighs 375g. The sensors are two Sony 1/3" progressive scan CCD (Color/BW). The sensors have selectable resolutions of 640x480 or 1024x768. Frame rate outputs are 640x480 at 30FPS or 1024x768 at 15FPS

5.4.4 Laser Distance meter

A laser distance meter is essentially a laser "tape measure" which measures the distance between two objects. In this application it would be used to accurately measure the distance between the rotor-craft and the ground. The range of measurement of such systems is 0.2 up to 200 m (0.7 up to 650ft) with an accuracy: ±1.5mm (0.06in). These meters are commercially available and are utilized successfully on existing UAV systems.

5.4.5 Sick Laser Ranger

The Sick Laser range finder (www.sick.com) is a non contact laser measurement system that scans its surroundings two dimensionally. It sends out an array of laser beams over it's field of view (typically 180 degrees), and – from the data received back from the laser beams – calculates distance and position for objects located in the field of view. There are several models of Sick Lasers. The Sick Laser flown by UC Berkeley (Figure 5.5) is a LMS-200 with a scanning range of 80 meters, and a nominal weight of 4.5 kg. It needs 24 V voltage, and consumes 20 W. It's dimensions are 156x155x210 mm. Note that while the weight of this sensor can be reduced some, carrying such a payload is a quite substantial task for an UAV.

Figure 5.5. UC Berkeley Yamaha RMAX with Sick Laser demonstrating obstacle avoidance. Image obtained from http://robotics.eecs.berkeley.edu/bear/index.html

5.4.6 Utilization of obstacle detection information

The previous sections discussed the possible sensors for obstacle detection. However, once data has been collected, it needs to be processed and then utilized. These sensors will collect data continuously at typical rates ranging from 1 to 10 Hz. Once a datapoint is collected it will have to go to a processing flow, which will trigger a possible action. Once this action has been triggered, the UAV will have to react to the action. Thus, in considering whether a sensor actually allows for effective obstacle avoidance we will need to consider the detection range, acquisition rate, UAV speed, processing time and reaction time. In order to consider all of these in the same units, we can transform the detection range into time by dividing it by the UAV speed. This will give the maximum window of time that our system should react in. For example, a detection range of 20 meters and a UAV speed of 4 m/second would translate into a maximum window of 5 seconds. Given the fact that reaction times of UAVs (to go from forward to stop) are typically in the order of 2 seconds (in which under the example at hand 8 meters would be covered) we can see that – as long as our obstacle avoidance system can process the information in less than 3 seconds we should be able to utilize the obstacle detection information effectively. Note that this assumes that we can convey this information effectively to the UAV control system. Based on discussions with UAV manufacturers (who provide many "hooks" into their control system this seems a reasonable assumption). Based on the current state of such systems (in which processing of the data happens near instantaneously) this assumption on processing time seems to be well within bounds.

5.5 Summary

The problem of obstacle avoidance for autonomous UAV operation requires the ability to accurately collect appropriate data on obstacles, process this data, and have the UAV react to this data. Based on the information discussed in this section and results from other UAV research groups, we conclude that effective obstacle avoidance can be feasibly be implemented on autonomous helicopter UAVs.

6 Magnetic signature associated with an UAV

6.1 Introduction

An effective UAV Magnetometer system needs to be able to collect magnetic data which will provide for the detection and identification of target ordnance. There are multiple aspects to this:

1. The need to collect data in close proximity to the target. The magnetic field of a magnetic target falls off as the inverse cube. Thus, if we increase our standoff from 1 meter to 2 meters, the signal will decrease by a factor of 8. This imposes the need to have our sensors as close to the ground as possible to detect small ordnance, as well as the need to obtain samples of the magnetic field at spatial intervals in the order of 5-10 cm.
2. The need for accurate data point positioning information
3. The need to collect intrinsic low noise magnetic data . It is possible in theory to eliminate the "platform induced" noise for handheld magnetometers (note that orientation and heading induced noise are in general not well addressed for handheld magnetometers). However, a helicopter (be it a manned or an unmanned system) will have a significant intrinsic magnetic signal produced by the materials from which it is constructed, as well as a rotor induced noise. In order for an UAV magnetometer system to be effective, this signal needs to be minimized to the fullest extent possible. The approach to this has two components
    a. Minimization of the signal by counteracting (degaussing, bucking) the magnetic signal of the platform and by creating a standoff between the platform and the magnetometer by mounting the magnetometer on a boom or similar structure, thus reducing the magnetic signal of the platform
    b. Software compensation of the remaining magnetic signal of the platform

In order to assess whether it is possible for an UAV magnetometer system to be effective, we performed a series of field measurements of the magnetic signal of a target UAV (the Neural Robotics Autocopter). These field measurements were accomplished using a set of two Geometrics G823A magnetometers. For all measurements data were collected using one magnetometer as a base station and the second magnetometer to sense the field associated with the UAV. This second sensor was placed in different configurations and positions with respect to the UAV, with and without the UAV engine running. The G823A magnetometers were calibrated and compared in tests without the UAV to verify that they performed correctly, and that they both tracked the diurnal variationto within the sensitivity of the systems. The heading error of these magnetometers (the effect of the orientation of the sensor on the recorded value of the magnetic field) was determined to be maximum 0.5 nT. This is in agreement with the manufacturer specifications.

Two series of tests are discussed here. The first one examines the effect of the orientation of the helicopter on the magnetic signal for different positions of the magnetometer with respect to the UAV. The second series of tests examines the effect of the engine noise on

the magnetic signal for different orientations of the magnetometer with respect to the UAV.

6.2 Effect of the orientation of the UAV on the magnetic signal

For this test the UAV was placed on a non-magnetic rotating platform. Initial tests showed that for acceptable levels of noise results we need to place the magnetometer on a boom in front of the UAV as mounting the sensor directly underneath the UAV results in effects of about 800 nT peak to peak over a 360 degree rotation.

Results shown here are for the magnetometer placed on a short boom (50 cm forward of the UAV) (Figure 6.3 top), and for the magnetometer placed on a long boom (120 cm forward of the UAV) (Figure 6.3 bottom). The expected variation in the UAV induced effect is that this would be inversely with the boom distance. The platform was rotated 360 degrees, and then returned to the original position by rotating 360 degrees back. During this rotation data was collected on a time base. Rotation was performed both with and without the helicopter on the platform, so as to be able to assess the effect of the UAV. While maintaining an identical rotation speed with and without the UAV was not possible, the graphs can be compared qualitatively to obtain an estimate of the UAV effect.

The rotation test was performed in an open area adjacent to the INL research facility. There are a number of buildings located within 1 to 2 hundred yards from the area of testing, so there is a fairly substantial gradient field in the test area. This is the purple line in figure 6.1 and 6.2. As expected, the longer boom shows the larger variation in the effect observed without the UAV.

The rotation of the platform with and without the UAV allows us to assess the relative magnitude contributed by the UAV. Rotation tests were done over a period of about 1 -2 minutes. Data from the base station is not shown here as this did not change more than approximately 0.2 nT over the measurement period, and does not change the interpretation of the results in any way. Figure 6.1 shows the yaw induced noise for the short boom, and figure 6.2 shows the yaw induced noise for the long boom. In all cases the data is shown normalized to the first measurement. Note that as the boom length increases the variation observed in the magnetic field increases from the short to the long boom, however, the sign and behavior of this field is the same. The start position and magnetometer orientation is the same in all cases. Figure 6.3 shows the different configurations for the short and the long boom.

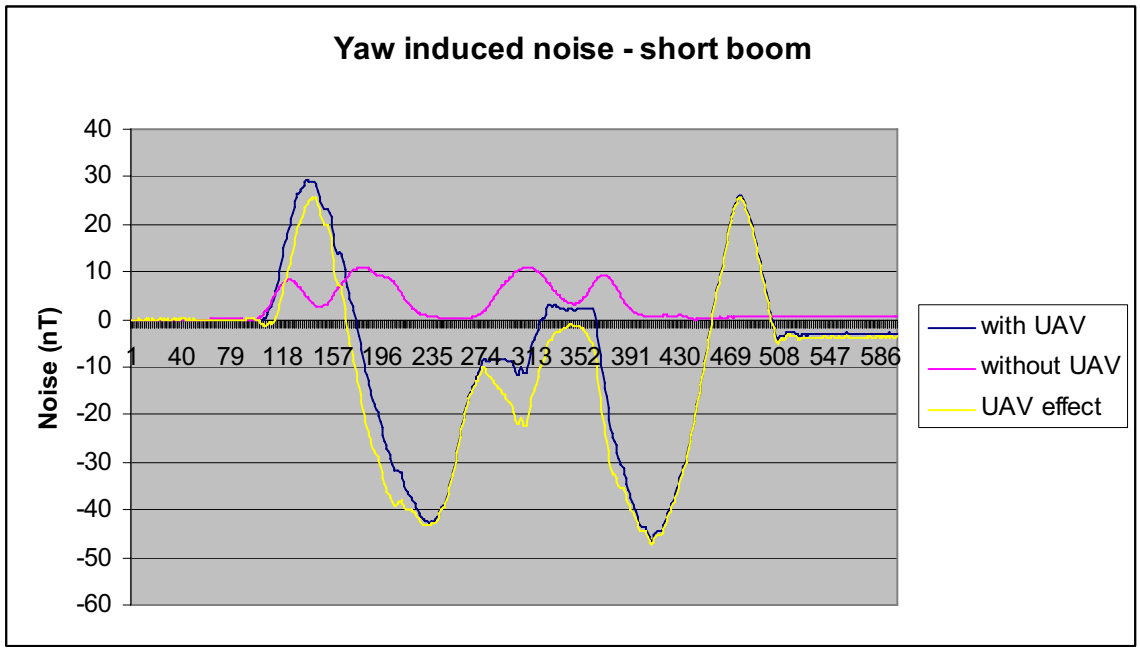

Figure 6.1 Yaw induced noise – short boom. The purple line is the natural gradient. The blue line is the gradient measured with the UAV. The yellow line is the approximate effect of the UAV. Peak to peak effect is about 80 nT. Note that the rotation is 360 degrees on way, and 360 degrees back. Data are plotted as a function of sample number. The negative peak at sample 235 corresponds to an 180 degree rotation.

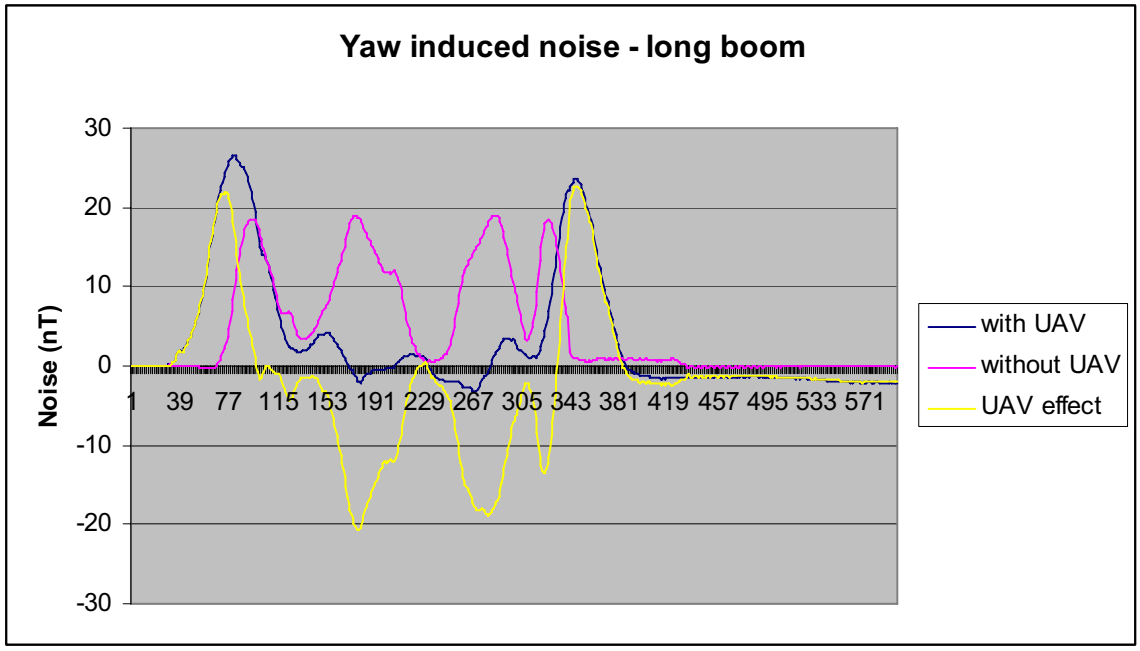

Figure 6.2 Yaw induced noise – long boom. The yellow line is the difference between the two measured dataseries. Peak to peak effect of the UAV is about 40 nT.

Analysis of the data from figures 6.1 and 6.2 shows that the effect of a 180 degree rotation of the UAV is about 40 nT (peak to peak) for the long boom, and about 80 nT for the long boom. It should be noted that these values are approximate as the rotation of the platform with and without the UAV was not precisely synchronized. However, the order of magnitude of these effects should be correct. This effect is one which can be corrected for assuming that the orientation of the UAV is known precisely, and assuming that we can characterize the UAV effect in "free space" (effectively by flying the UAV in the different cardinal directions at elevations of several hundred feet above the ground). Assuming that the yaw angle is known to within two degrees, we can conservatively expect that we can reduce the noise associated with the yaw effect to about 1 nT for the short boom, and 0.5 nT for the long boom. It should be noted that active magnetic compensation of the platform is expected to reduce the magnetic signature of the platform substantially, which will also reduce the magnitude of the yaw induced noise.

Figure 6.3. Yaw test setup. **Top**: short boom. **Bottom:** long boom. Setup allows 360 degree rotation of platform.

6.3 Effect of the UAV motor and rotor

In addition to the yaw tests, a series of tests were done to determine the effect of the rotor and engine noise on the UAV. These tests were done on a UAV runway in the desert, approximately 50 miles west of Idaho Falls. The UAV runway consists of asphalt

emplaced on top of native bedrock. Apart from the asphalt there are no buildings, pipelines, power lines or any other structures within 4 miles of this site. We thus expect to have very low ambient magnetic noise. For these tests, the UAV was strapped onto a non-magnetic (PVC) platform which can be moved back and forth over a PVC track. Data were collected for a range of different configurations: all systems turned off, electrical systems turned on (but engine not running) and the engine running, with rotor speed ranging from low (idle) to about 1500 rpm (take off rotor speed). Data were collected in the same manner as in the previous system (base station placed in a fixed position, about 60 meters from the UAV, and measurement sensor placed adjacent to the UAV).

Figures 6.4 and 6.5 and 6.6 show some detail of the setup.

Figure 6.4. Setup for UAV motor noise test. The INL UAV runway is located several miles from any infrastructure, about 50 miles west of Idaho Falls. Stand on left contains basestation. Stand on right shows helicopter on rolling non-magnetic frame. Data from both magnetometers is recorded at center setup.

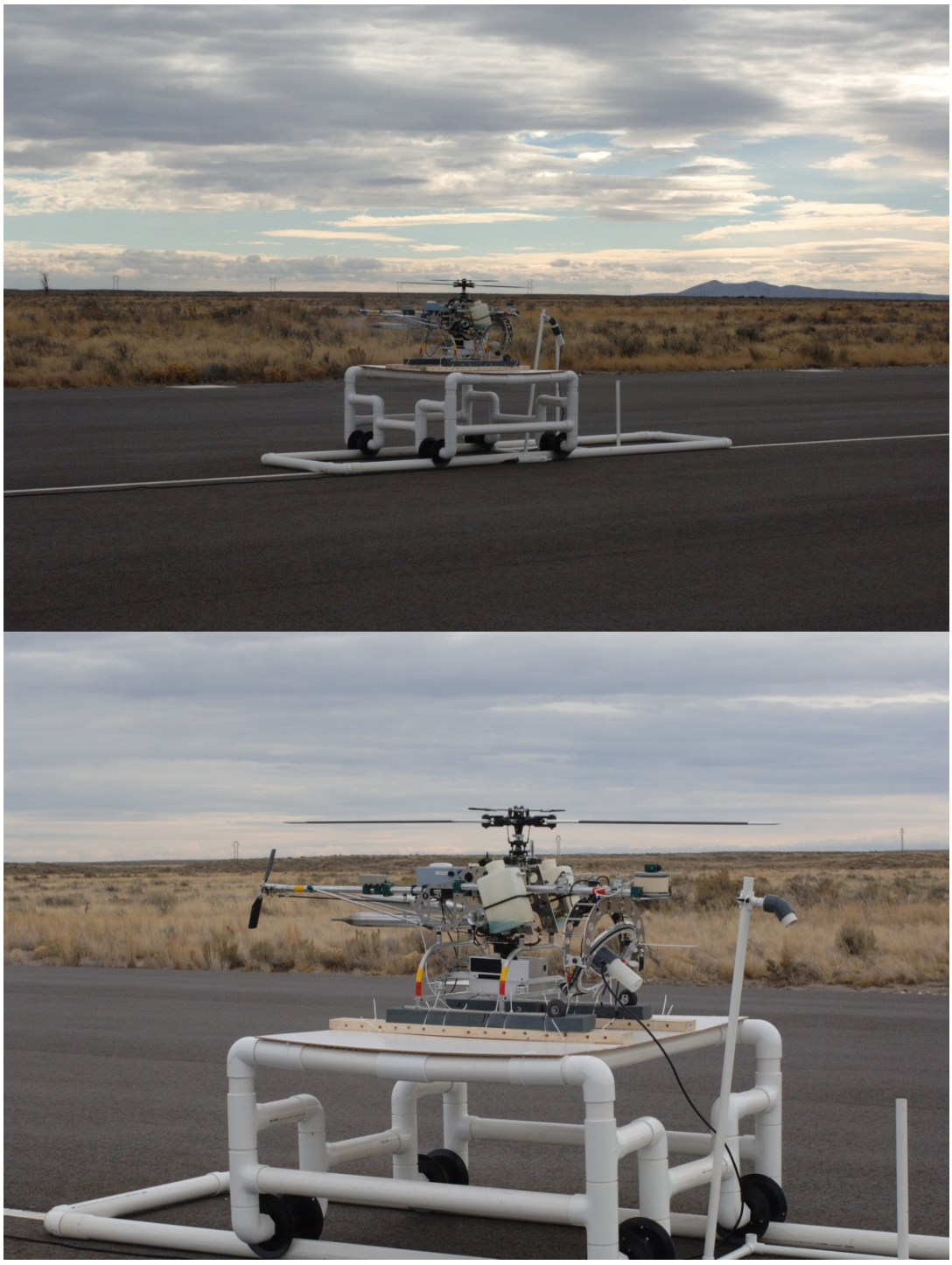

Figure 6.5. Detail of helicopter mounts. The Helicopter is strapped to foam pads mounted on a non-magnetic PVC frame. The frame can be moved over a PVC track. 6.5 **top** shows front mount (magnetometer 80 cm in front of airframe). 6.5 **bottom** shows camera mount (magnetometer mounted in camera gimble). Note: bottom figure also shows holder for front mount. Front mount would correspond to location of magnetometer placed on a boom.

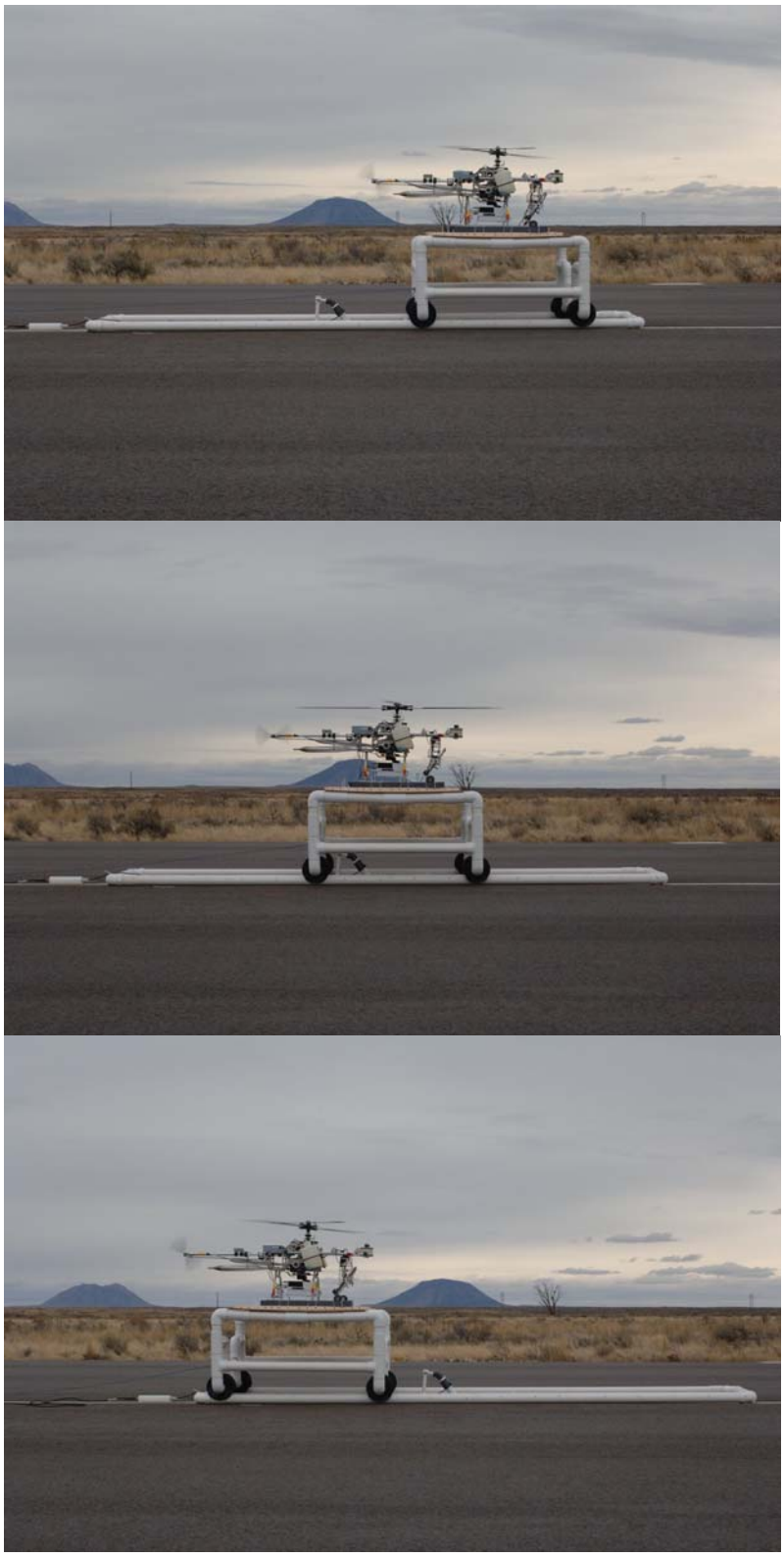

Figure 6.6 Images from pullover test showing location of magnetometer. The magnetometer position is fixed, while the UAV (with motor running at 1500 rpm) is moved over the magnetometer. During these tests the top of the magnetometer sensors is 77 cm below the skids

of the helicopter.

Data was collected for a range of different configurations, both with the motor on and with the motor off. In addition, the effect of the electronics being turned on was evaluated. In general, the electronics being turned on or off do not change the signature, and – as expected – we observe a DC effect from the airframe, and an oscillatory effect from the rotor effect.
The datasets discussed below include a subset of these configurations. Other datasets essentially confirm the observations which can be made from these datasets. The configurations discussed here include

- sensor mounted in *front mount* (figure 6.5, **top**)
- sensor mounted in *camera mount* (Figure 6.5, **bottom**)
- sensor mounted in *bottom mount* for a pull over test (Figure 6.6)

Data are generally shown relative to the first measurement taken in a series, which removes the effect of any DC offset. Data are shown as a function of measurement number. Data acquisition rate is 10 Hz.

6.3.1 Sensor mounted in camera mount

Figure 6.8 shows the data for the sensor mounted in the camera mount. Figure 6.8 topFor this, the motor was revved up, and then kept at take off rotation speed (1500 rpm) from about measurement 500

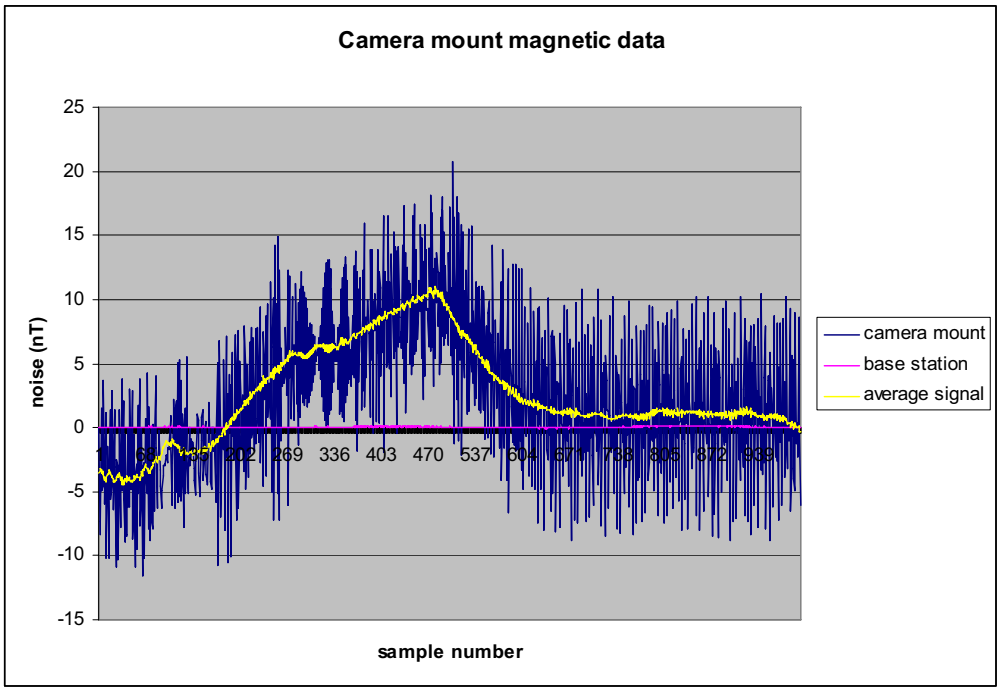

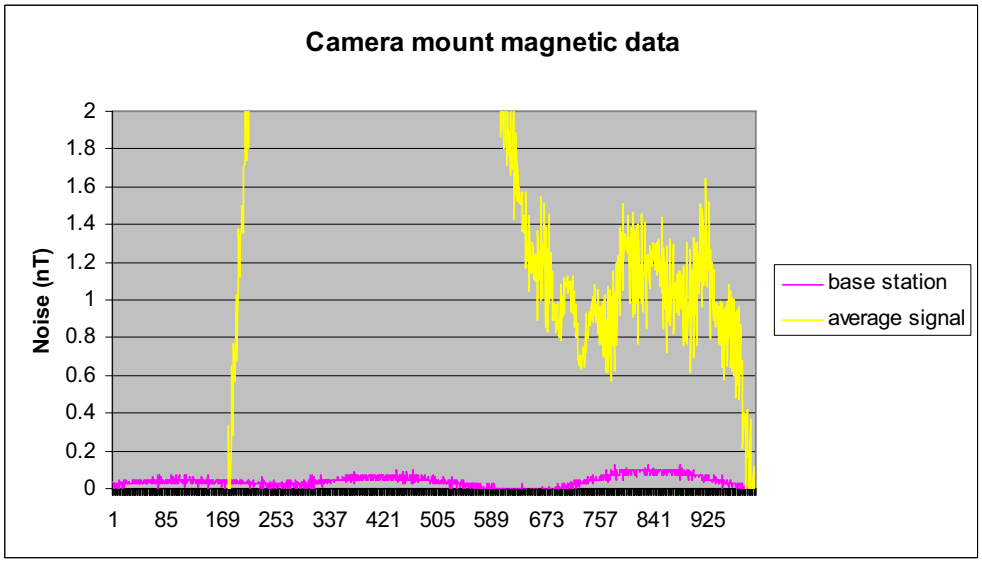

Figure 6.8 Rotor induced noise for camera mount (Figure 6.5, bottom). Different noise levels for idle (first few hundred measurements), revving up (up to measurement 550), and full throttle (1500 rpm – measurement 600 onwards). Top shows both raw, averaged and base station data. Bottom figure shows averaged data and base station. Data is averaged using a running window over 20 measurements.

6.3.2 Sensor mounted in front mount

Figure 6.9 shows the data for the sensor mounted in the front mount (Figure 6.5, top). For this, the motor was revved up, and then kept at take off rotation speed (1500 rpm) from about measurement 100

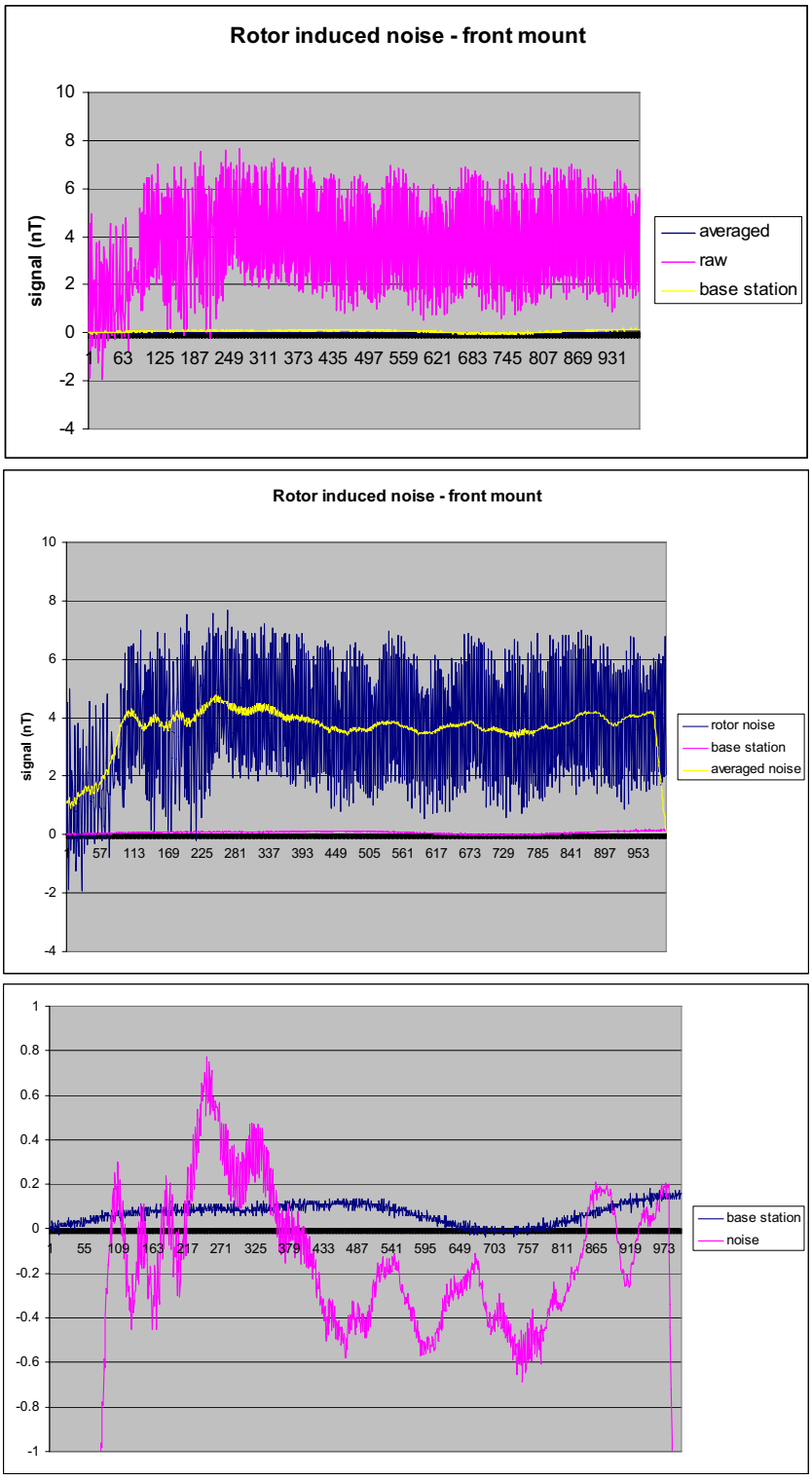

Figure 6.9. Raw, averaged and base station data for rotor induced noise for front mount. Data is collected at 10 Hz. Averaging window is 2 seconds. Data shown at bottom is same as data shown in top, but with raw data removed and DC shift applied to show match between base station and averaged data. Averaging reduces the noise by factor of 4

From the data shown in figure 6.8 and figure 6.9 we can make the following observations

1. For the camera mount the rotor-induced noise is about 15 nT peak to peak.Averaging of this data can reduce the noise to about 1 nT peak to peak, but does not show a clear correlation with base station variations
2. For the front mount the rotor induced noise is about 4 nT peak to peak. Averaging of this data reduced the noise to about 1 nT peak to peak. The averaged signal does not show an obvious correlation with the base station data

One point which is noteworthy is that we observed (and expect) vibration effects for the camera mount. While we made an effort to reduce this effect, there was a noticeable effect, which is increased due to the fact that the UAV is strapped down.

6.3.3 Data from pullover test

For the pullover test the sensor was placed on the ground in the center of the PVC track and the UAV (with the motor running at 1500 rpm) is pulled over the sensor in one feet increments (Figure 6.6). The raw data for this test is shown in figure 6.10. The data shows both a DC effect, and a high frequency noise effect.

In order to quantify the high frequency noise effect, the data was corrected for each of the intervals by applying an offset, and averaged using a 7 point filter. The results of this are shown in figure 6.11, which shows a close match between the base station signal and the averaged, dc shifted signal.

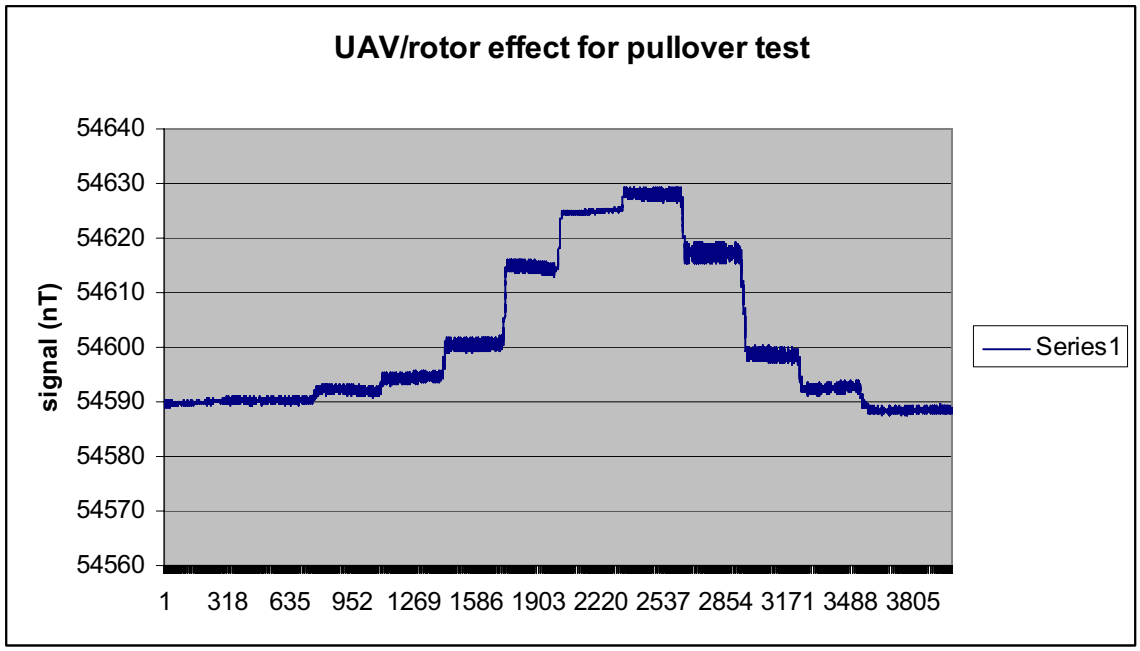

Figure 6.10. Data from pullover test showing effect of combined UAV/rotor for pullover test. This effect is a combination of the static UAV effect and a high frequency rotor effect.

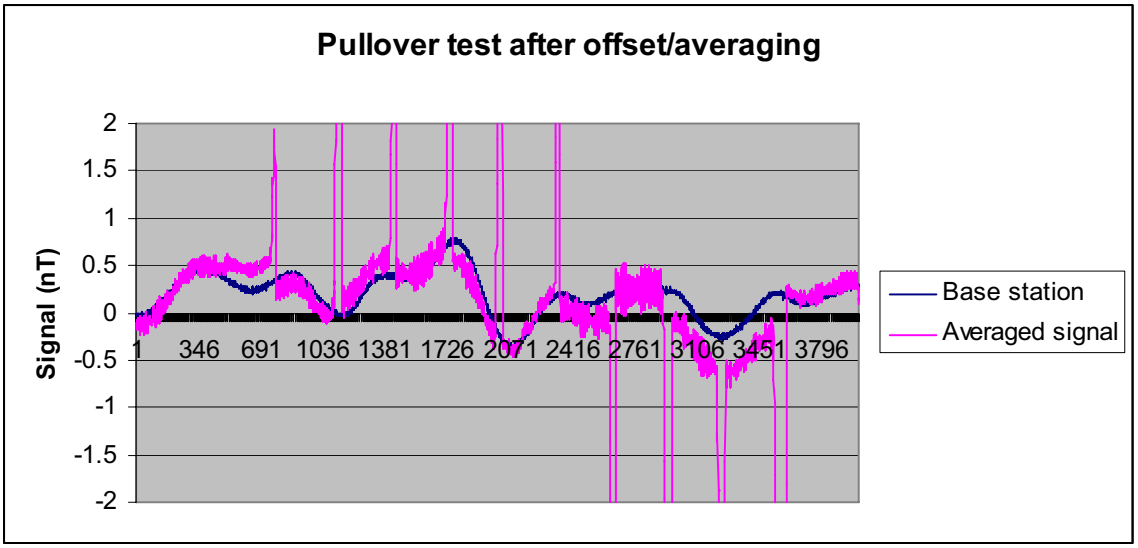

Figure 6.11 After applying an offset to each of the intervals (remove DC signal from UAV) and averaging the rotor noise (7 sample averaging window) the averaged signal closely matches the basestation data in shape. Peaks correspond to transition between intervals.

The results of this series of tests indicate that the rotor-induced noise can be minimized to about 0.2 nT through application of a simple filter.

6.4 Compensation of moving-platform magnetic systems

Platforms carrying magnetometers may have magnetic fields comparable to or larger than the ones the sensors are intended to measure. Thus, some type of calibration and removal of the platform's field is generally essential to obtaining useful magnetic measurements. The only viable alternative is to place the sensor at a significant distance from the platform, which often creates logistical problems, other sources of error, or both.

Fortunately, the dominant components of the platform field can often be analyzed in relatively simple terms. The critical simplification is that the collective effects of similar sources at the sensor are all that matter. Thus, it is unnecessary to analyze separately the fields originating in the engines, fuselage, etc., unless these vary in ways that affect the field at the sensor differently.

To illustrate, consider first the simplest of fields, those due to permanently magnetized components of the platform. As long as these do not change with time, their summed effect at any location, including that of the sensor, is a constant vector. Thus, these effects create a simple bias in a vector sensor. However, for the total field sensors under consideration here the measured anomalous field is (approximately) the projection of the field onto the earth's field direction. Since the permanent fields are fixed in the

platform's reference frame and not that of the earth, the anomalous field is a function of the platform orientation.

To analyze this effect, consider the components of the constant vector in the aircraft reference frame – *T* directed starboard, *L* directed forward, and *V* directed upward. Then if *cos X* is the earth's field with respect to the starboard direction, *cos Y* with respect to the forward direction, and *cos Z* with respect to the upward direction, then the anomalous total field due to the permanently magnetized components is

$$\Delta T_P = T\cos X + L\cos Y + V\cos Z.$$

As the platform changes its orientation, the direction cosines change and so does the anomalous total field effect. However, the behavior of this change with respect to orientation is fixed, so analysis of data obtained from platform maneuvers to extract this component should enable it to be predicted and removed. This is the basis of most forms of compensation.

The second well-known source of platform noise results from the earth's field acting on the magnetically permeable components of the platform. For any such component, the effect is proportional to the earth's field vector in the platform reference frame, and each component of this vector results in a magnetic disturbance vector at the sensor location. Thus, the effect has the form of the matrix product of two vectors. This produces an overall constant of proportionality equal to the earth's field intensity, and a three by three array of coefficients which depend on the magnetic permeability of the platform component and the products of the direction cosines of the earth's field with respect to the platform reference frame.
Since this effect has the same form for all components of the platform, again only the sum is important, and is described by a three by three array which can be estimated empirically by analyzing a set of platform maneuvers (calibration flight).

The third common source of magnetic platform noise is the magnetic field due to eddy currents resulting from changes in orientation of the conducting components of the platform in the earth's field, i.e., the Faraday effect. These noise sources are proportional to the earth's field vector and to the rate of change of the direction of the conductor with respect to the earth's field. Again, only the summed effect at the sensor location is important, so these effects are described by a three by three array of terms with proportionality factors which include the intensity of the earth's field, the direction cosines of the field with respect to the platform reference frame, and the rates of change of these cosines.

In practice, there may be numerous other important sources of magnetic platform noise. A particularly common one is magnetic fields due to current-carrying conductors in the platform. These may be wires or, in the case of ground returns through the frame, the chassis of the system. To the extent that these currents do not vary with time their effects may be combined with those of the permanently magnetized parts of the system. However, if this is not the case the effects of currents must be dealt with separately.

Generally speaking, this involves direct measurements of the currents and calibration of the changes in the field at the sensor with current variations.

One class of platform interference that generally cannot be calibrated and subtracted from the measured data is the magnetic field of rapidly moving parts, such as helicopter rotors. To remove these from the data it is necessary to sample the magnetic field rapidly enough that the noise signal is not aliased, and then notch-filter in the band in which the interference occurs. The data can then be down-sampled to a rate appropriate to the requirements of the signal of interest. That this approach is feasible is shown in the results discussed under section 6.3.

Figure 6.11 shows the fluxgate data used to compensate a total field magnetometer as previously described. The red trace is the *X* component measurement, the green trace the *Y* component measurement, and the blue trace the *Z* component. As would be expected for normal aircraft maneuvers, the *X* and *Y* components change sign, while the *Z* component does not.

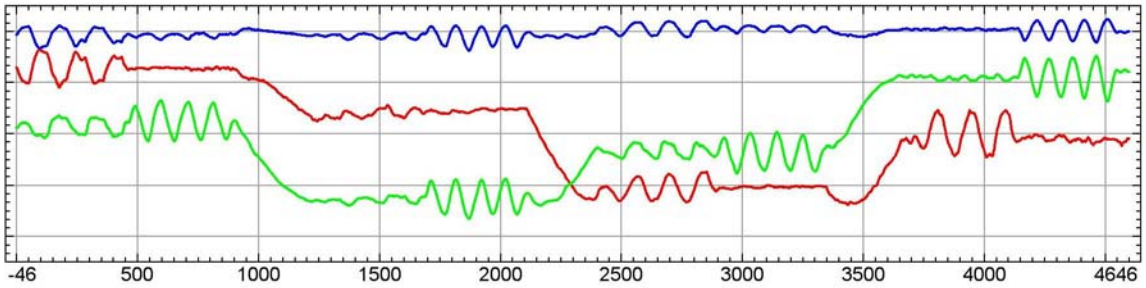

Figure 6.11. Fluxgate data used to compensate the total field. Vertical scale is +/- 50000 nT.

Figure 6.12 shows the uncompensated total field in red and the compensated field in green for the same maneuvers as in Figure 1. To exaggerate the maneuver signal, a high-pass filter has been applied to both traces.

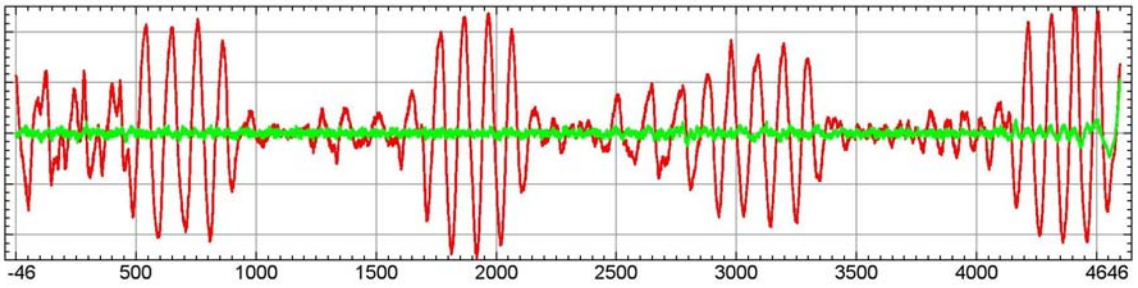

Figure 6.12. High-passed total field before and after compensation

6.5 Summary

The tests discussed in this section show that the UAV has a significant magnetic signature, both DC and AC. The DC magnetic signature of the UAV can be reduced significantly by placement of compensating magnets and replacement of some components. However, in order to collect data of sufficient quality, we will need to mount the magnetometer on a boom. Based on current measurements, a boom length of about 1 meter should be sufficient to collect data which – after correction – should be of sufficient quality to be used for target detection. The rotor creates a high frequency noise, which to a large effect can be removed through simple averaging or digital notch filtering. The rotor associated noise for suggested boom lengths (after simple filtering) is on the order of 0.5 nT. More advanced filtering approaches (using either magnetic fields sampled at frequencies of several hundred Hz, or multiple magnetometers) is expected to be able to decrease this noise significantly.

7 Summary and next steps

7.1 System feasibility

In section 2 we defined the challenges which needed to be resolved to be able to create an autonomous UAV helicopter magnetometer system. In sections 3-6 we discussed the results of our evaluation of these challenges

The conclusion of these evaluations is that – while it is by no means trivial to do so –an effective and operational autonomous UAV helicopter magnetometer system can be built.

After consideration of current UAV candidates, and consideration of the advantages of having multiple magnetometers as well as an advanced obstacle avoidance system, we feel that a system which can carry 3 magnetometers on a boom and a Sick laser would be a near ideal choice. Such a system would require a larger UAV than the Autocopter used in the tests described in this report (either an Autocopter XL or Yamaha RMAX or a similar system). This larger UAV would have operational flight times in the order of several hours. The expected cost of the Autocopter XL and the experience of the INL robotics group with this platform (around $40K) leads us to argue for this platform. An estimated cost of the payload for such a system is in the $60- $80 K range.

We feel that in order for such a system to be useful, it will need to have full autonomy. To us this implies that operators would indicate areas to survey and the system would take off, survey, and return for refueling. Such a system would have on board intelligence allowing for automatic grid refinement, as well as transmit data to a ground based system allowing near real time target characterization and identification.

7.2 Relative performance of manned vs. unmanned systems

A question which has not been addressed so far is the relative performance of the system proposed here to a manned system. This will obviously be a consideration in making the decision on whether it makes sense to proceed with an autonomous UAV system. While an in depth discussion of the relative merits of manned and unmanned systems falls outside the scope of this report, we feel that it is useful to present a brief discussion on this topic.

In order to be able to perform a comparison one needs to consider the scenario for which these systems should be used. The first scenario is one in which our objective is to – as completely as possible - characterize small targets (~1 lbs) for which we need to have flightlines which are similarly spaced to the standard separation between airborne magnetometers in an array (1 – 1.5 m) (Figure 7.1a). The second scenario is one in which our objective is to detect large targets (100-1000s of lbs). Under the second scenario our flightlines can be spaced tens of meters apart (Figure 7.1 b). Note that these two scenarios

are the two end members of the application of magnetic airborne surveying, and are used here to indicate relative performance of the systems. For WAA surveys the primary interest is in the small target scenario, and this is the scenario which should be considered for evaluating the relative merits of an UAV vs a manned helicopter system.

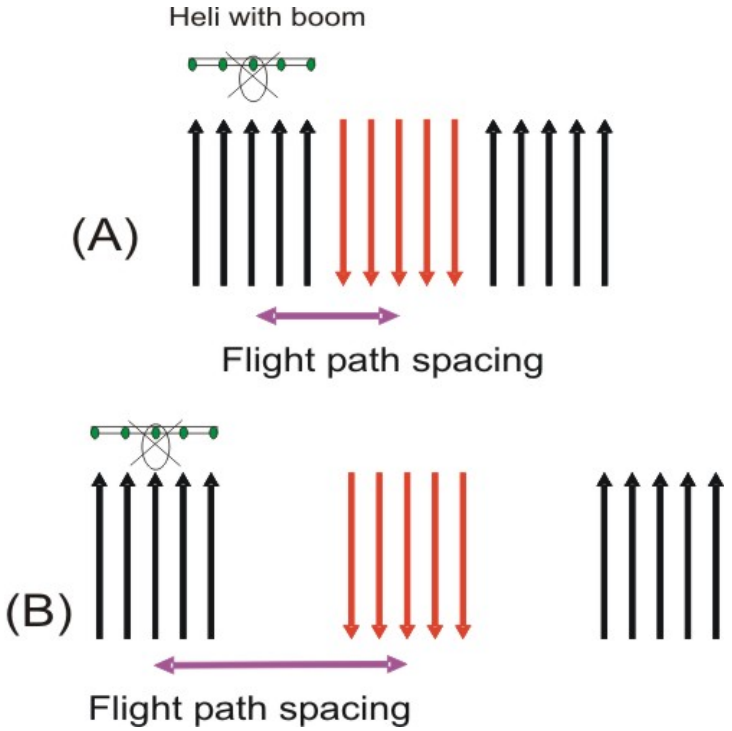

Figure 7.1 (A): flight path spacing for small target surveying (B) flight path spacing for large target spacing

Considering these scenarios, and system values which are relatively representative of current manned and projected unmanned systems we can create table 7.1. It should be noted that several of the values in table 7.1 are approximate, especially the cost per acre for unmanned systems.

The cost estimate is based on the fact that

- Back end processing costs are relatively similar per acre
- UAV has a much lower mobilization/demobilization cost
- UAV has a much lower O&M (two person operation)
- UAV has ability to survey smaller sites cost effectively
- An UAV has the potential ability to deal with a broader range of terrains than manned systems.

Note that while we can provide a likely cost range the exact operational cost a UAV system will only become clear from real field efforts.

It should be noted that the performance of an UAV system for large targets would be much closer to that of a manned system due to the similarity in flight path spacing. As

noted previously, for most WAA surveys the small target spacing will be the relevant scenario.

	Manned system	Unmanned system
System cost (K)	1000	120
Flight elevation (meters)	3	3
Speed (m/s)	15	7.5
Speed (knots)	30	15
Number of magnetometers	7	3
Sensor spacing (m)	1.5	0.5
Array width (m)	9	1
Flight path spacing (small target)	9 meters	1 meters
Theoretical time for 1 acre (seconds) (small target)	29	529
Cost per acre ($)	100-150	20-50 (??)
Flight path spacing - large target (1000 lbs)	70 meters	60 meters

Table 7.1 Comparison between manned and unmanned system. For the path spacing we assume that this is equal to the array spacing. Note that this assumes a fair amount of precision in positioning. However, current results of autonomous UAVs show that this precision is feasible.

Table 7.1 provides part of the story. However, as mentioned in section 1, performance includes cost, performance and operator risk. Table 7.2 summarizes our observations on these three factors. Thus, while we feel that one of the advantages of an unmanned system is the cost, a potentially more compelling argument is that an unmanned system takes the operator out of harms way – and allows for adaptive, data driven surveying.

	Manned system	Unmanned system
Risk to operator in case of crash	High	Low
Cost/acre	~$150	~$50
Performance	Good, but limited by operational constraints (fixed survey properties)	Possible to dynamically adapt survey behavior in reaction to data

Table 7.2 Cost, performance and risk comparison of manned vs. unmanned systems

7.3 Next step: a prototype autonomous UAV helicopter - magnetometer system

Given the results provided in sections 3-6, as well as the performance evaluation in section 7.1 the team assembled for SERDP SEED 1509:2206 feels that the logical next step would be the construction of a prototype autonomous UAV helicopter-magnetometer system. It should be stressed that assembling such a system is not a simple assembly effort of components, and thus we propose a structured, modular approach. In this approach, we recognize that there are several go/no go conditions (including e.g. UAV platform availability, obstacle avoidance at realistic speeds and the ability to accommodate the magnetometer boom). We also recognize that the exact specs for such a system require significant user community involvement, which would define requirements on type of terrain which would need to be surveyed, define average sites of areas to be surveyed, survey characteristics and so on. Based on these considerations, we propose that such an effort would follow the following scope and schedule:

Year 1

- In depth determination of system performance specs (user community driven)
- Sensor and boom development

Year 1 - 2

- Obstacle avoidance implementation/refinement/testing
- Autonomous system selection and integration with manufacturer for payload/interface modifications

Year 2

- On board processing development

Year 2-3

- Fieldtesting and cost/performance analysis
- Coupling with control and interpretation package and development of turnkey system

Such an effort would be performed with the same team as assembled for the effort described in this report. We would anticipate working in close collaboration with a commercial UAV manufacturer in phase 2, and would anticipate a significantly larger role for the DoD teammembers, who would be key in both defining user needs and in the field validation efforts.

8 Appendix 1: contact information

Roelof Versteeg
Idaho National Laboratory
PO Box 1625
Idaho Falls, ID
Phone: 208 526 4437
Fax: 208 526 2639
Cell: 208 569 1606
email: roelof.versteeg@inl.gov

Mark McKay
Idaho National Laboratory
PO Box 1625
Idaho Falls, ID
Phone: 208 526 0539
Fax: 208 526 7688
email: Mark.McKay@inl.gov

Matt Anderson
Idaho National Laboratory
PO Box 1625
Idaho Falls, ID
Phone: 208 526 4308
Fax: 208 526 7688
email: Matthew.Anderson@inl.gov

Ross Johnson
Geometrics, Inc
2190 Fortune Dr.
San Jose, Ca. 95131 U.S.A.
Phone: 408-428-4242
Cell: 408-515-0266
Fax: 408-954-0902
Email: ross@geometrics.com

Bob Selfridge
U.S. Army Corps of Engineers
ATTN: CEHNC-ED-CS-G/Selfridge
4820 University Square
Huntsville, AL 35816-1822
Telephone: (256) 895-1887
Fax: (256) 895-1602
E-mail: Bob.J.Selfridge@hnd01.usace.army.mil

Jay Bennett
Environmental Systems Branch
Ecosystem Evaluation and Engineering Division, Environmental Laboratory
U.S. Army Engineer Research and Development Center
3909 Halls Ferry Road
Vicksburg, Mississippi 39180
Email: Jay.Bennett@erdc.usace.army.mil,
Phone: 601 634-3924

9 References

Chapuis, J., C. Eck, H. P. Geering and H. Allenspach (1997). Autonomously Flying Helicopter. 4th IFAC Symposium on Advances in Control Education, Istanbul, Turkey.

Doll, W. E., T. J. Gamey and J. S. Holladay (2001). Current Research into Airborne UXO Detection. SAGEEP Annual Meeting, Oakland, CA.

Gamey, T. J., W. E. Doll, L. P. Beard and D. T. Bell (2003). Analysis of noise coherence in airborne magnetic gradients for UXO detection. 2003 SAGEEP Meeting, San Antonio, TX.

Gamey, T. J. and R. Mahler (1999). A Comparison of Towed and Mounted Helicopter Magnetometer Sys tems for UXO Detection. SAGEEP 1999, EEGS.

MIT (1998). MIT Entry in the 1998 International Aerial Robotics Competition. IARC, Hanford, WA.

Nelson, H. H., D. L. Wright, T. Furuya, J. R. McDonald, N. Khadr and D. A. Steinhurst (2004). MTADS Airborne and Vehicular Survey of Target S1 at Isleta Pueblo, Albuquerque, NM, 17 February - 2 March 2003, Naval Research Laboratory.

Salem, A., T. J. Gamey, D. Ravat and K. Ushijima (2001). Automatic Detection of UXO from Airborne Magnetic Data using a Neural Network. Proceedings of the 2001 Symposium on the Application of Geophysics to Engineering and Environmental Problems, Denver.

Stanley, J. M. (2003). Approaching 100% Quality Assurance in Ferrous Explosive Ordnance Disposal. Armidale, Australia, Geophysical Technology Limited**:** 10.